Journal of Constructional Steel Research 206 (2023) 107936

Contents lists available at ScienceDirect

Journal of Constructional Steel Research

journal homepage: www.elsevier.com/locate/jcsr

Truss imperfections in the design of bar and diaphragm bracing systems

Natalia Korcz-Konkol *, Piotr Iwicki

Gdańsk University of Technology, Faculty of Civil and Environmental Engineering, Department of Engineering Structures, Gabriela Narutowicza 11/12, 80-233 Gdańsk, Poland

ARTICLE INFO

Keywords:
Roof bracing
Diaphragm
Imperfection
Stabilizing force
Stressed-skin effect

ABSTRACT

In the article three variants of roof bracing were considered: bar bracing, diaphragm bracing and the combination of bar and diaphragm bracing. Different analytical and numerical ways of taking into account the imperfections of the truss girder were compared. The entire 3D model of the roof (shell and beam elements with the eccentricities taken into account) was analysed numerically. Selected stressed-skin aspects were considered. Stabilizing forces in the purlins and forces in bracing elements (bar and/or diaphragm bracing, connections) were observed. The importance of the imperfection issues (e.g. shape of the imperfection, method of including imperfection, wind forces) was evaluated numerically to indicate the key points in the design procedure. The biggest forces in purlins occurred for "nonstandard" shape of the imperfection. On the other hand, in case of bracing elements, when wind forces were taken into consideration, "standard" approach of including the imperfection was safe approximation. Moreover, the diaphragm took over significant part of the bracing forces, however the distribution of the forces depended strongly on the flexibility of the bracing and purlin/truss connection.

1. Introduction

Steel structure parts, such as trusses, beams or frames, are designed to carry loads in their plane. These elements have much greater strength and stiffness in the plane in which the main load is applied than in the perpendicular direction hence should be protected from out-of-plane buckling by using bracing. One of the example is transversal roof bracing which carries not only wind-induced loads, but also loads due to imperfections of the truss girders. These imperfections can have various origin (geometrical, material). According to Eurocode 3 [1], the effect of all types of imperfections can be reflected by means of equivalent geometric imperfection with appropriate magnitude.

The influence of the imperfections of the restrained elements on the bracing system can be taken into account in different ways. The most popular approach, proposed in [1], is to assume the bow shape of the initial imperfection of the restrained element and replace it by the equivalent stabilizing force. Thus avoiding the direct modification of the "ideal" geometry of the structure in numerical analysis what simplifies the design procedure. However the calculations have to be run including second order theory (iteration or geometrically nonlinear analysis need to be performed). In [2–4] the assumptions of Eurocode 3 [1] are discussed and alternative procedures of calculation the imperfection-induced forces in bracing system are suggested.

Other possible way to take into account the imperfections is direct implementation in numerical model. The "ideal" geometry of the structure can be modified e.g. by using selected forms of the instability (elastic buckling modes). Although this approach seems to reflect the nature of the phenomenon best, it is also more complicated and hence not popular in engineering practice. However, it has been used in many scientific studies concerning imperfections, e.g. in the analysis of the stability of roof trusses [5].

Typical roof of steel structure consists of girders/trusses, purlins (optionally), bracing and cladding (e.g. trapezoidal sheeting or sandwich panels). In [6] three classes of the structure depending on the function of the cladding are distinguished. Class I is the case where sheeting effects the resistance and stability of the main bearing structure, class II – the case of interaction of the cladding only with secondary elements and class III – the case of considering only covering function of the cladding.

Stiffening effect of the cladding on the structure resulting from the in-plane (shear) resistance and stiffness of the sheeting is called "stressed-skin effect" (or "diaphragm effect"). The basic stressed-skin design rules concerning sheeting are presented in ECCS recommendations [7]. Although this theory was born in the 1960's, the stressed skin

* Corresponding author.
E-mail addresses: natalia.korcz@pg.edu.pl (N. Korcz-Konkol), piwicki@pg.edu.pl (P. Iwicki).

https://doi.org/10.1016/j.jcsr.2023.107936
Received 9 January 2023; Received in revised form 13 March 2023; Accepted 28 March 2023
Available online 8 April 2023

theory and design methods are still being investigated. In [8] the modification of the analytical formulas for calculation the flexibility of the diaphragm was proposed. Another researches concentrated on developing of the numerical manners to take into account the diaphragm effect [9–11]. The parametric study of the influence of the cladding on the stability of the structural elements together with the comparison between proposed numerical design models was presented in [12,13]. Simplified numerical models of the trapezoidal sheeting and connections were compared in [14,15]. Finally, the unwanted (so-called "parasitic") stressed-skin effect was pointed in scientific discussion as the alarming phenomenon occurring in existing structures, especially in big sheds, which requires the adjustment of the existing procedures and numerical approaches [11,16–18]. When the diaphragm effect is omitted by the designer, but acting in real structure, the leakage or even failure can occur. The behaviour of the small-scale diaphragm and the selected modes of failure were observed in experimental investigation in [19]. The failure modes of bigger diaphragm was observed in experimental research in [8].

The analyses of the alternative procedures of calculation the stabilizing forces acting on bracing system [2–4] concern the case of the roof consisting of truss girders, purlins and bar bracing. Sheeting is assumed not to be a part of the primary structure and the diaphragm bracing is not within the scope of that analyses. In the studies concerning the trapezoidal sheeting as a bracing, usually only the influence on the resistance and stability of the bearing elements (e.g. trusses, purlins) is considered [5,6,20]. When stressed skin theory is taken into account, typical case is loading perpendicular to the side wall of the building [7]. Very few references guiding how to design the diaphragm bracing under gable bracing loads (wind loads acting perpendicular to gable wall) and rafter bracing second order forces [7,21,22] can be found. Procedures to determine the stabilizing effect of the sheeting on rafters and the effect of the sheeting on purlins are provided in [7,22], however the equivalent geometric imperfections of the restrained rafter in the design of the diaphragm bracing system of purlin roof are not commented. Recognising this issue, authors started to investigate the behaviour of the structure with imperfections and the trapezoidal cladding acting as a diaphragm. First observations were described in [23], were it was confirmed that the distribution of the stabilizing forces differed from the values obtained according to [1] and the stiffness of the bracing affected the forces in purlins, similarly to [24].

For the purpose of this paper, part of the steel single-storey building roof consisting of truss girders and purlins was analysed in three variants of bracing. In first case, called BBr, bar bracing were considered and the corrugated sheeting was neglected. Second case, called DBr, considered diaphragm bracing with the assumption that trapezoidal cladding – apart from "traditional" covering function – is also the component of a bracing system and acts as a shear diaphragm. In third case, called BDBr, structure with both trapezoidal cladding and bar bracing was analysed, which corresponds to the combination of bracing systems (bar and diaphragm). It can be conscious choice or can occur beyond the will of the designer.

The article presents the observation of the imperfection-induced forces important in the design procedure: forces stabilizing the upper truss chord and forces in bracing elements (bar and/or diaphragm bracing, connections). The main objective of this research is to evaluate the importance of the truss girder imperfections in reference to transversal and diaphragm bracing of the roof with purlins in order to indicate the key points in the design procedure.

Imperfections of the truss girder were analysed numerically and compared to the analytical methods. Geometrically nonlinear analysis of the bracing systems were conducted by means of Abaqus software [25]. Selected innovative elements were addressed, such as the entire structure of the roof, eccentricities between elements and flexibility of selected diaphragm components. In analytical procedures known from literature one shape of the initial imperfection of the upper truss chord is taken into consideration. Simultaneously, factors as e.g. assemble process may cause another shape of the imperfection too. The possibility of occurrence of the imperfection shapes other than represented by the first buckling mode were noticed also in [26]. In this paper, four exemplary shapes of initial imperfection of the truss girder were considered.

2. General description of the analysed structure

The studied structure was a part of the pitched roof consisting of three trusses, purlins and bracing elements (bar and/or diaphragm), as presented in Fig. 1. The main characteristic of the roof structure followed the publications [5,23,27]. The trusses length was 24 m and spacing was 6 m. The depth of the trusses was non-uniform (1.61 m in the middle and 0.9 m at the supports). The upper truss chord was made of 2L90×90×9 profile with the connection between L profiles using 14 battens (180×74×5 mm plates) supplied at midpoints between truss joints. The bottom truss chords were made of 2L 80×80×8 profile. Diagonals near the supports were made of 2L65×65×7 profile and the other diagonals - U65 profile. *Z*-purlins (Z250×65×2) were located every second truss joint with 2.39 m spacing and connected with the upper truss chord using angle cleat (vertical leg - 0.235 m, horizontal leg - 0.055 m, thickness – 0.008 m, length - 0.165 m). The yield strength of the steel assumed in the analysis was $f_y = 350$ MPa, the modulus of elasticity was 205 GPa and the Poisson's ratio in elastic stage was 0.3.

Three bracing systems were considered (see Fig. 1): bar bracing (BBr), diaphragm bracing (DBr), and bar and diaphragm bracing (BDBr). In BBr case the X-shaped bracing (flat bar bracing members - 30×4 mm) was taken into account. In DBr case the trapezoidal sheeting with the cross section presented in Fig. 2 was assumed part of the bracing system. The fastening to the purlin was realised in every trough in the centreline of the corrugation (210 mm spacing between screws). In case BDBr the trapezoidal roof cladding was considered a structural element together with flat bar bracing. The corrugated sheeting was the same as in case DBr and the cross-section of the flat bar was 30×4 mm again.

Cases DBr and BDBr were analysed in two variants: "a" and "b" (see Fig. 1b,c,e,f). In variant "a" the sheeting was included only in the area of bar bracing in BBr case. This variant was used for the analysis of stabilizing forces. In variant "b" the sheeting was covering whole area of the roof. This variant was used additionally for the analysis of forces in bracing elements. Bar bracing case (BBr) was also considered in two variants: "a" and "b". In BBr_b case of the analysis, purlin transverse bracing made of C150 cold-formed profiles was additionally included (see Fig. 1a,d).

3. Analytical calculations of the stabilizing forces

Selected analytical methods of calculations the stabilizing forces in purlins were described in [23]. These information is quoted below for the clarity of the article.

3.1. Standard method -"EC" procedure

Eurocode 3 procedure [1] to calculate the equivalent stabilizing force based on two main assumptions:

- the initial geometrical imperfection of the restrained element is the parabolic bow imperfection with maximum value $e_0 = \alpha_m L/500$, where: L – the span of the restrained member, α_m – the coefficient taking into account irregularity of the geometrical imperfections of restrained m members $\alpha_m = \sqrt{0.5(1 + 1/m)}$,
- the compression force $N_{Ed,i}$ in the restrained element i is constant.

The equivalent stabilizing force can be calculated as $q_{EC} = \sum 8N_{Ed,i}(e_0 + \delta_q)/L^2$, where: $N_{Ed,i}$ – maximum compressive force in the restrained element i, δ_q – in-plane deflection of the lateral bracing system

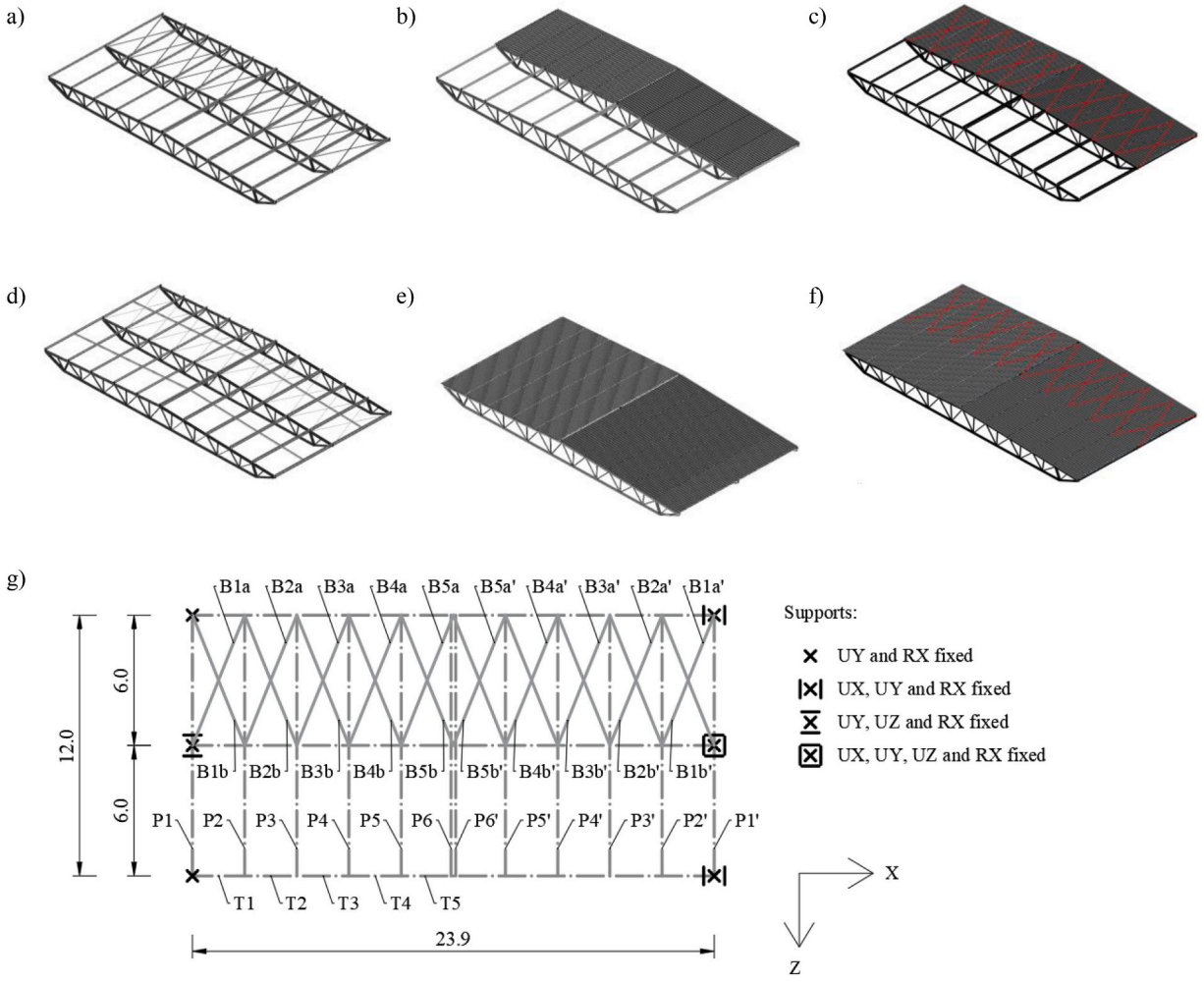

Fig. 1. Roof structure: a) BBr_a case – analysis of purlins, b) DBr_a case – analysis of purlins, c) BDBr_a case – analysis of purlins, d) BBr_b case – analysis of bar bracing, e) DBr_b case – analysis of diaphragm bracing, f) BDBr_b case – analysis of bar and/or diaphragm bracing, g) main dimensions and numeration of the roof elements: purlins (P), upper truss chord elements (T), bar bracing members (B). Note: Bar bracing covered in a view by the sheeting are marked in red. (For interpretation of the references to colour in this figure legend, the reader is referred to the web version of this article.)

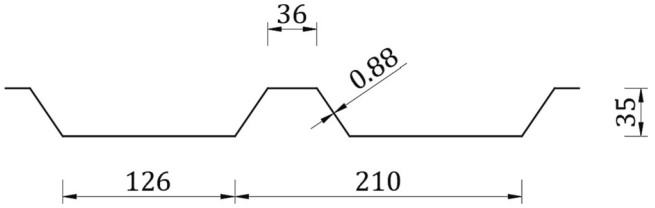

Fig. 2. Trapezoidal sheeting cross-sectional geometry [mm].

in the mid-span caused by q_{EC} and all other external loads (e. g. wind load) obtained from the first order analysis; in case of the second order analysis $\delta_q = 0$ may be assumed. Finally, the force in one internal purlin due to the equivalent stabilizing force q_{EC} can be calculated as $F_{EC} = q_{EC}a$, where a is the purlin spacing.

3.2. Alternative method - "q and H" procedure

– In [2] the alternative approach of calculating the equivalent stabilizing force is presented. This method for the purpose of this article was called "q and H" procedure. In the contrary to [1], non-constant value of the compression force in the restrained member is taken into account, according to quasi-parabolic formula: $N_{Ed}(x) = 4N_{Ed,i}\frac{x}{L^2}(L-x)$. The shape of the second order parabola of the geometrical imperfection is assumed: $y(x) = 4e_0\frac{x}{L^2}(L-x)$. Finally, the equivalent force q_2 can be calculated as: $q_2(x) = 16N_{Ed,i}\frac{e_0}{L^2}\left(6\frac{x}{L} - 6\frac{x^2}{L^2} - 1\right)$.

In the "q and H" procedure it is noticed that the upper chord is not isolated from the truss as it is assumed in [1]. Therefore, it is proposed to take into account additional component of the equivalent stabilizing force due to the distortion of the truss girder (resulting from the initial bow imperfection of the upper chord): $H_2(x) = y(x)\frac{P}{h} = 4Pe_0\frac{x}{hL^2}(L-x)$, where: h - the height of the truss, P - value for vertical force in the joints of the truss (reactions from the purlin).

3.3. Alternative method - "F and H" procedure

In [4] another alternative approach of calculating the stabilizing forces in purlins is presented. This method for the purpose of this article was called "F and H" procedure. Similar to [2], two components of stabilizing forces are considered. The stepped-changing character of compression force in the imperfect upper chord is taken into account. The difference between this method and "q and H" procedure is in the approach to calculation of the stabilizing forces due to compression. According to "F and H" procedure the force in each next purlin is

calculated using the formula (components defined in Fig. 3): $F_{\varphi,n+1} = N_n \sin\varphi_n - N_{n+1}\sin\varphi_{n+1}$. The calculation of the second component of stabilizing forces – due to distortion of the truss girder is the same as in [2].

4. Numerical analysis - model description and methods

4.1. General description of the structure

Numerical analysis of the structure built according to section 2 was conducted in Abaqus software [25]. Truss chords and diagonals, purlin-chord connectors and trapezoidal sheeting were applied as S4R shell elements (4-node shell with reduced integration), see Fig. 4.

Purlins were applied as B31OS beam elements (2-node linear open-section beam), which was a modification compared to the analysis presented in [23]. Using beam elements instead of shell elements simplified significantly the model and the interpretation of the forces in purlins. Local effects, which disturb axial results in purlins, such as the contact interaction between upper flange of the purlin and bottom flange of the sheeting or between the web of the purlin and the connector in the purlin-truss connection, were neglected. Simultaneously, the axis of the purlin beam element was established in the middle of the web height and placed in the numerical model taking into account the eccentricity between purlin and other elements of the structure (Fig. 4a). In order to evaluate the use of beam elements instead of shell for the purpose of the stabilizing forces observation, one variant of the analysis (DBr with equivalent stabilizing force q calculated according to [1]) was modelled in two ways. Axial forces obtained in "beam" purlins were compared with the axial forces in "shell" purlins (calculated based on the average stresses in the cross-section of the purlin) and satisfactory correspondence has been achieved. Next, global deformation in the direction of the wind loading in the midspan of the third truss in selected variant of the analysis was checked. The discrepancy was observed, what was commented in the context of the results in section 6.4.

Bar bracings were applied as B31 beam elements (2-node linear beam), which was also a modification compared to the analysis presented in [23]. Based on the forces in purlins and bar bracing it was concluded that using for bar bracing beam elements instead of shell does not influence significantly results, however simultaneously reduces complexity of the model.

Connection between bar bracing and the truss was simplified - end nodes of bar elements were coupled to the central nodes of the angle cleats (Fig. 4e). Truss elements (diagonals and chords) were connected using tie connection between small end area of the particular elements.

4.2. Stressed-skin aspects in numerical model

According to [7] shear flexibility of the diaphragm is due to sheet deformation, connections deformation and flange forces. In case of roof with purlins following connections are specified: sheet-purlin fasteners, seam fasteners (sheet-sheet fasteners) and connections to rafters – purlin-rafter connections and shear connections (if exists). The analysed structure was designed without shear connectors, which is a common practise.

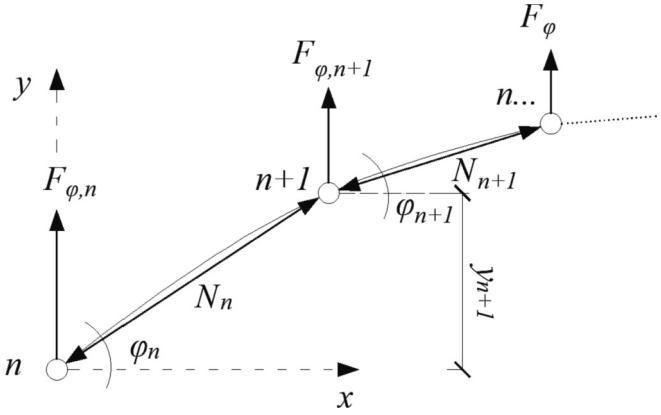

Fig. 3. Scheme of the stabilizing forces in purlins calculation described in [4].

Sheet deformation results from profile distortion and shear strain. Both forms were included in current analysis thanks to modelling steel trapezoidal sheeting using shell elements which allowed to reproduce the exact cross-sectional and planar geometry of the sheeting. Profile distortion is more complex issue, depending not only on diaphragm geometry. It is also influenced by the location of the sheeting to purlin fasteners (in every/alternate troughs, central/side position in the trough [15]) and by the length of sheets. The location of the sheeting to purlin fasteners was included in the current analysis (described further). Trapezoidal sheeting was treated as one structural element, not as the assembly of sheets connected by seam fasteners, so the length of particular sheets was not reflected, nor was the flexibility of seam fasteners.

Fasteners (screws) which connect bottom flange of the sheeting and top flange of the purlins were taken into account in the analysis by means of bushing connections [25]. Bushing elements were defined between nodes on the bottom flange of the sheeting and nodes at the axis of the purlin, so the scheme of the fasteners was mapped (elements were in the exact place of the screws). What is more, the flexibility characteristic of the connection was included. Tension stiffness and rotational stiffnesses (bending and torsional) were calculated based on the geometry of the fastener. The most significant stiffness in diaphragm effect - the stiffness in the plane of the diaphragm (in two directions) - was calculated based on the slip value of the screw with neoprene washer equal to 0.35 mm/kN [7]. The operation of bushing element was examined based on the small model consisted of two parts: shell instance and beam instance, connected by the group of bushing elements. The stiffness and the forces in elements met the analytical expectations.

Purlin-truss connection was realised using angle cleats (Fig. 4) and built using shell elements. The horizontal part of the connector was tied to the chord (shell to shell constraint) and the vertical part was coupled to the purlin (four nodes of the L-shaped connector, which mapped the group of bolts, were tied to the node of the purlin – Fig. 4d). Due to use of shell elements the main component of the flexibility of this connection (the flexibility of the angle cleat) was included. However the purlin was built from beam elements, so the torsional deformation of the purlin (due to the local effect of the connection upper flange of the purlin and bottom flange of the sheeting) was omitted.

According to stressed-skin theory, roof sheeting acts as a deep plate girder. This results in flange forces in the edge members of the diaphragm. In case of the analysed load scheme sheeting spanning was parallel to the length of the diaphragm, so the flange forces occurred in upper truss chords. When the wind load acts on gable frame, the effective depth of the "in thought" plate girder equal to 2/3 of the width of the roof is suggested in [21] for uninsulated building with purlins. Following this formula, in case of the analysed structure the maximum range of the diaphragm action was 16 m, which covered three trusses. Remembering that the diaphragm action exists between edge members, depth corresponding to three trusses (12 m) was assumed safely. The truss was built using shell elements and the eccentricities between all structural elements of the roof were included, so this component of the shear flexibility of the diaphragm was taken into account.

4.3. Boundary conditions and load scheme

The scheme of the truss supports together with main dimensions and elements of the structure is presented in Fig. 1g. Rigid/free supports were used instead of elastic supports to limit the number of variable factors of the analysis. Self-weight of the trusses were taken into account as gravity load applied to all truss elements. Snow load and self-weight

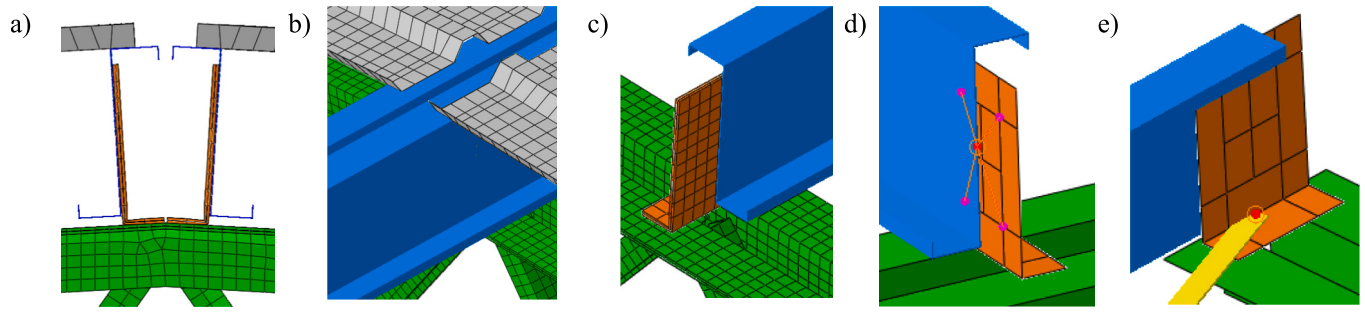

Fig. 4. Details in numerical model: a) ridge with two purlins – view 1, b) ridge with two purlins – view 2, c) purlin-truss connection, d) coupling between angle cleat and purlin, e) tie between angle cleat and bar bracing. Note, that the *Z*-shape of the purlin and flat bar is just the visualization of the beam element cross-section.

of the rest of the roof (purlins, sheeting and connectors) were assumed equal to 2 kN/m^2 and were applied as the reaction forces from the purlins to the trusses in every second truss joint with the value $P = 28.68$ kN in internal joints and $P/2 = 14.34$ kN at the eave joints (see Fig. 5). Reaction forces instead of area loading were applied in numerical model in order to discount the effect of the purlin and sheeting loading which would make the issue more complex and the results unclear. Reactions were applied to the horizontal parts of the angle cleats (purlin-chord connectors) as traction in the gravity direction. Load scheme ensured compressive forces in the top chord of the truss (restrained element), what was the condition to observe the stabilizing forces. Additionally, in the analysis of forces in bracing elements, wind acting on gable wall was considered. Assuming wind load equal to 0.8 kN/m^2 and the average height of the wall equal to 8 m, the reaction wind forces exert from the gable columns into the roof with the value $W = 7.65$ kN (and $W/2 = 3.82$ kN at the eave joints). Wind load was applied to the centre points of the purlin-chord connectors as point loads. In BBr case taking into account the wind load leaded to the high values of forces in purlins. It was identified that transverse bracing in the midspan of the purlins should be included in numerical model in order to obtain appropriate behaviour of the elements of the structure (see Fig. 1a,d).

Main load schemes are presented in Fig. 5. It should be noted, that gravity loading presented in Fig. 5 was taken into account only in models with initial imperfections included directly in the calculations and was omitted in models regarding imperfection as equivalent stabilizing force q.

4.4. Initial imperfections

Initial imperfections of the chosen truss girder (the gable one, bottom in Fig. 1g) implemented directly in numerical model were obtained from the Linear Buckling Analysis (LBA). In LBA purlins were disconnected from the chosen truss which allowed for the eligible deformation of the truss. Then, buckling modes were exported from the results. Next, meshes with the selected imperfection shapes were imported to the target model so that the static analysis including geometrical nonlinearity was possible. The LBA results were used in order to include in the analysis the deformation of the whole truss girder (as it may occur in reality), not only the deformation of the fictively isolated chord (as in analytical solution [7]). Imperfection modes chosen to the analysis are presented in Fig. 6. Shape 1 (Fig. 6a) was a bow imperfection of the upper truss chord and corresponded to the absolute value of the lowest value of critical load. This shape was close to the "classic" imperfection (taken into account in analytical procedures), however the shape of the upper chord was not ideally parabolic (it was a result of the LBA, so the exact shape could not be dictated). Moreover, the top chord was not isolated, but the whole truss was deformed (also diagonals and bottom chord). Shape 2 (Fig. 6b), was the bow imperfection of the bottom truss chord. In this case, again, it was not ideal parabolic bow shape and the chord (in this case - bottom) was not isolated, but the whole truss was deformed. Analyses of idealised imperfections corresponding to two above shapes can be found in literature [1–4] Comparison of the analytical and numerical results was presented in section 5. Shape 3 (Fig. 6c) was an example of the two-half-wave imperfection of the upper

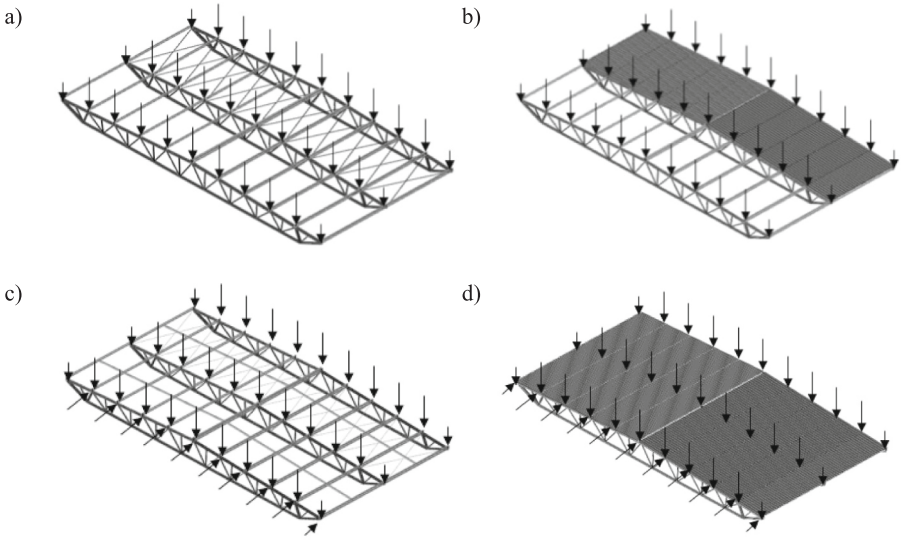

Fig. 5. Main load schemes: a) BBr_a case – analysis of purlins (with gravity loading), b) DBr_a or BDBr_a case – analysis of purlins (with gravity loading), c) BBr_b case – analysis of bar bracing (with gravity and wind loading), d) DBr_b or BDBr_b case – analysis of bar and/or diaphragm bracing (with gravity and wind loading).

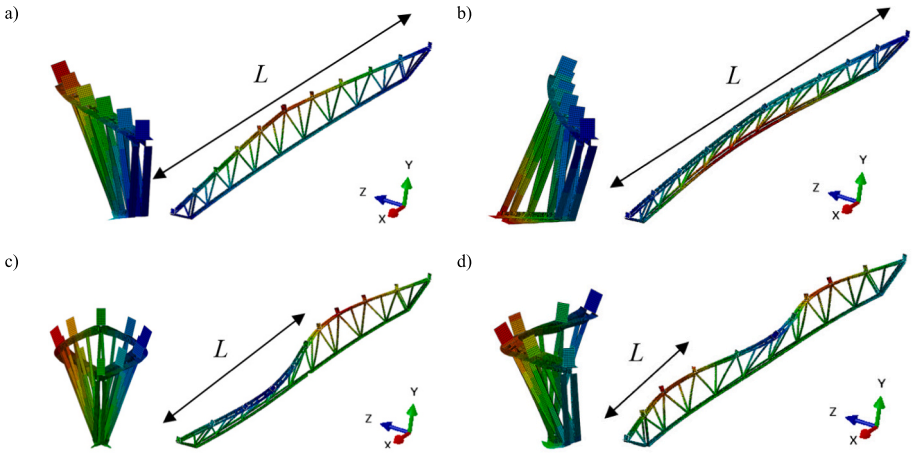

Fig. 6. Initial imperfections of the truss: a) Imp1 ($e_0 = -L/500 = -48$ mm), b) Imp2 ($e_0 = L/500 = 48$ mm), c) Imp3 ($e_0 = L/500 = 24$ mm), d) Imp4 ($e_0 = L/500 = 16$ mm).

truss chord. Taking into consideration the fact that the truss is usually the assembly of two halves, this shape of the initial imperfection seems to be possible too as the sum of two "classic" bow imperfections. What is more, this shape can occur as a result of using temporary struts in the middle of the truss girder span (which fix the girder in the middle of the span) during the assemble process until the rest of the neighbouring structure is built in. Shape 4 (Fig. 6d) was a three-half-wave imperfection of the upper truss chord. The imperfection in this shape can occur during assemble process if the truss cord is fixed in two points along the span (for example by temporary struts or longitudinal bracings).

The imperfection magnitude e_0 was adopted according to section 3.1. Taking into account the shape of the imperfection in relation to the length of the analysed element (truss), the span of the restrained element L was interpreted as the length of the half-wave of the imperfection shape (see Fig. 6).

5. Results and discussion of analytical and numerical calculations – axial forces in purlins

The analysed structure was built following the publication [23] and the main geometry of the roof, cross-sections of the structural elements and gravity loading in both analysis were the same. This fact allowed to use in current research the values of the compression forces $N_{Ed,i}$ in the elements of the upper truss chord provided in [23]. Forces were obtained in geometrically nonlinear analysis for the structure without implementation of the initial imperfection of the truss. Calculation of the forces was based on the average stresses obtained in every chord element T*i* in the cross-section close to the truss joints. Values in one half of the truss were read (T1-T5 elements in Fig. 1) and the symmetry was assumed (what was the approximation). Other assumptions varied depending on the analytical method, as follows:

- "EC3" procedure [1] – constant compressive forces with the value obtained numerically for the chord element T5 ($N_{Ed,i} = cons = N_{Ed,5}$),
- "q and H" procedure [2] – quasi-parabolic compressive forces with the maximum value equal to the value obtained for the chord element T5 ($N_{Ed,\max} = N_{Ed,5}$),
- "F and H" procedure [4] – compressive forces obtained in numerical analysis.

The difference between values of compression forces $N_{Ed,i}$ achieved in two ways – as parabolic imperfection ("q and H" procedure) and directly in numerical calculations ("F and H" procedure) - was between 0% (chord element T5) and 19% (chord element T1) [23]. The equivalent stabilizing forces calculated according to formulas described in section 3, are presented in Fig. 7 (q_{EC} – Eurocode 3 method and q_2 - "q and H" procedure).

Then, the axial forces in purlins were obtained applying formulas from section 3. The results calculated according to "EC" method and two alternative analytical methods are presented in Fig. 8. The pitched roof was considered, so there were two purlins in the ridge (no. 6 in Fig. 1). That is why the values for "P6×2" in Fig. 8 are the doubling of the force in one purlin no. 6. The assumptions about compressive forces in the restrained element (very close value of the compressive force in the midspan of the truss) caused practically the same values of the forces F_i in purlins P6. However the differences in F_i values in other purlins occurred. The discrepancies between "EC" analytical method and alternative method "$q + H$" resulted directly from the differences in the distribution of the equivalent stabilizing force along the truss (Fig. 7). The attention should be also paid to the distortion of the truss girder which results from the initial bow imperfection of the upper chord and should be considered as the extra forces H_i according to alternative procedures. In both alternative approaches H_i values are equal. In Fig. 8 they were presented in separate column, however the final force acting in purlin is the sum of forces F_i and H_i – as presented in further figures. In EC procedure this issue is not considered.

Three cases of the roof bracing systems were the subject of the numerical analysis: bar bracing (BBr_a), diaphragm bracing (DBr_a) and the combination of bar and diaphragm bracing (BDBr_a). Geometrically nonlinear analysis of the structure with imperfect geometry was performed and axial forces in purlins were observed. What is more, the "perfect" structure was analysed. In order to evaluate the outcomes related to imperfection only and eliminate forces with other origin, axial forces in purlins in case of "perfect" model were subtracted from axial forces in case of "imperfect" structure. Following analysis concerns the difference of the values. Values were read in the cross-section in the middle of the purlin length.

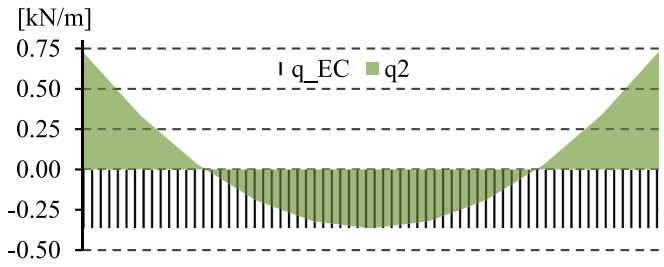

Fig. 7. Equivalent stabilizing force along the truss girder for two analytical methods.

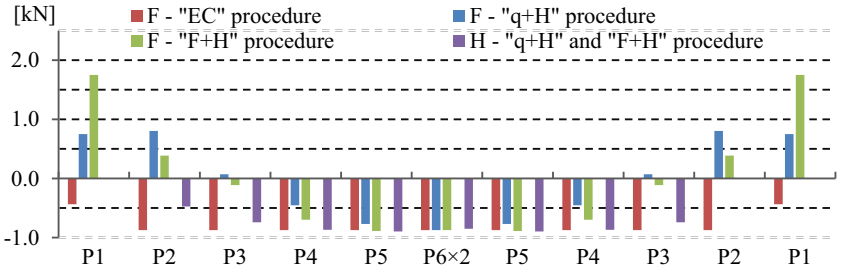

Fig. 8. Components of axial forces in the purlins resulting from initial imperfection of the upper truss chord – EC3 and alternative analytical methods.

Values of the axial forces in purlins calculated analytically and numerically are shown in Fig. 9-10. Note, that all axial forces results presented below concern the variant "a" of the cases (see Fig. 1). The reason for that modification (compared to the analysis presented in [23]) was that in this variant the sheeting did not influence directly the purlin forces in the area close to the imperfect truss, so the results (stabilizing forces) were more clear. Finally, in current analysis the lack of the symmetry of the structure was not omitted and can be noticed in numerical results. This asymmetry resulted from, among others, the asymmetry of static scheme (see Fig. 1g), automatic generation of FE (mesh) and mesh-related constraints.

In Fig. 9 axial forces in purlins obtained in case of bar bracing (BBr_a) for different initial imperfections are presented. Comparison between variant "EC" (values from analytical calculations) and "force q" (values from numerical analysis – the structure loaded by force q calculated based on "EC" method) confirmed that the way of read and interpretation of the stabilizing forces in purlins was correct (the difference did not exceed 16%). The distribution and the extreme forces depended on the imperfection shape and other assumptions of the method of including in the analysis imperfection forces. The biggest force values were obtained for the shape no. 3 of the imperfection (more than 2.5 times larger than in analytical EC calculations), then for the shape no. 4 of the imperfection (more than 1.5 times larger than in analytical EC calculations). The differences were observed, although the magnitude of the imperfection was adapted taken into consideration the shape of the imperfection (see section 4.4). This fact suggests that shape no. 1 should not be assumed arbitrary in the analysis of bracing systems and the consideration of the real shape of the imperfection may be required.

In Fig. 10a axial forces in purlins obtained both in analytical and numerical analysis for the shape no. 1 of the imperfection are presented. Numerical computations confirmed the shape of the stabilizing force distribution, which differed from the distribution according to analytical Eurocode calculations ("EC3") - purlins were not only under compression, but also under tension in the area close to the support. However the extreme values of the forces according to numerical analysis were significantly smaller than according to alternative analytical methods (although still about 30% higher than results according to EC).

In Fig. 10b-d axial forces in purlins obtained for the imperfection with the shape no. 2, 3 and 4 are presented. The stabilizing axial forces in purlins depended strongly on the shape of the imperfection, but only slightly on the case of the bracing (bar and/or diaphragm).

6. Results and discussion of numerical calculations – bracing elements

Initial imperfections affect not only purlins, but also other structural elements of the roof bracing. In order to design the roof bracing system, forces in bracing elements need to be known. Second order forces (which are the result of the initial imperfection of the restrained and compressed element) are only one of the bracing loading components. The second one, which is in fact the main load of the roof bracing system, is wind acting on gable wall.

6.1. Axial forces in bar bracing elements

Presented analysis concerned two cases when bar bracing occurred – bar bracing case (BBr) and bar and diaphragm bracing case (BDBr). X-shaped bracing with the numeration of the bar elements is presented in Fig. 1g.

Firstly, values of the axial forces in bar bracing elements which are the results of the second order forces only were observed. The analysis was conducted for bar bracing case (BBr_a) and included both equivalent force q and four selected shapes of the initial imperfections. Results are presented in Fig. 11. Selected deformed shapes of bar bracings are presented in Fig. 12. The outcomes showed that loading the structure by stabilizing force q (calculated according to EC3) resulted in bigger axial forces in bar bracing than in cases of implementing initial imperfection directly in the model. It means that the EC assumptions were safe for the analysed structure. On the other hand, comparison between two responding cases – "force q" and "imperfection no. 1" (both were based on similar shape of the initial imperfection) pointed that the EC approach was very conservative (almost 2 times difference in extremal axial force occurs), so the question arise if this level of the safety is necessary. Also the distribution of the axial forces in the bracing elements in case of imperfection no. 1 differed significantly from the values obtained in accordance with EC 3 procedure (the extreme axial forces occurred in other bracing elements). In Fig. 11 another aspect is clearly visible – the initial imperfection with the shape no. 1 caused much

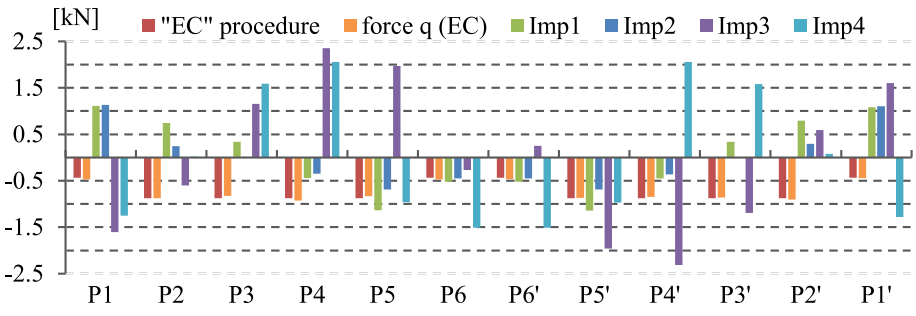

Fig. 9. Axial forces in purlins – BBr_a case.

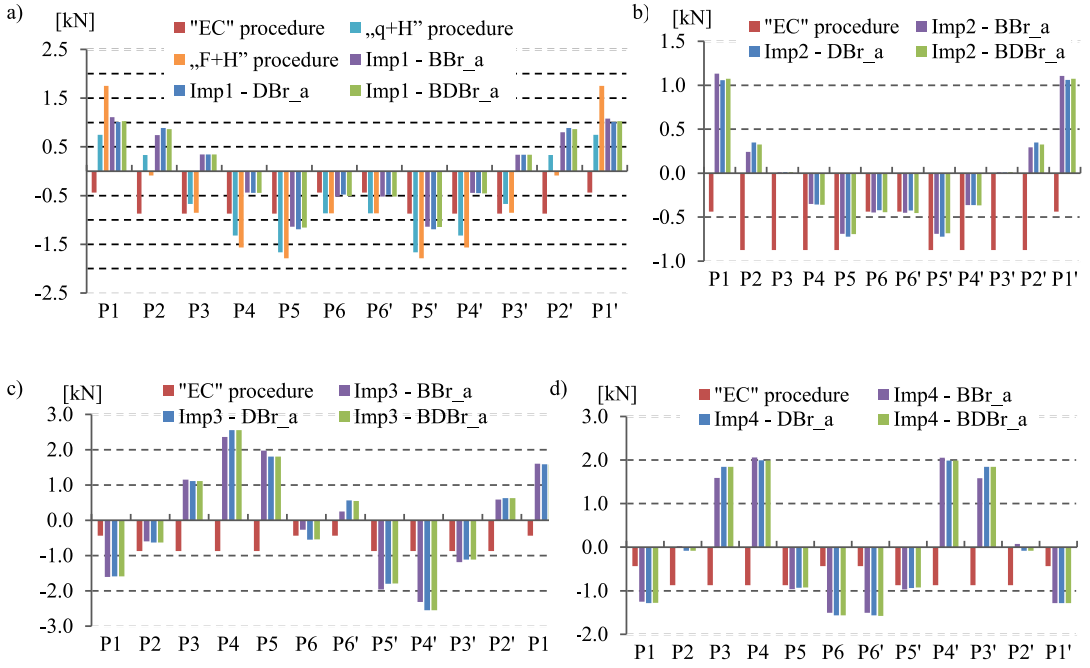

Fig. 10. Axial forces in purlins: a) Imp1 (comparison of analytical and numerical results), b) Imp2, c) Imp3, d) Imp4.

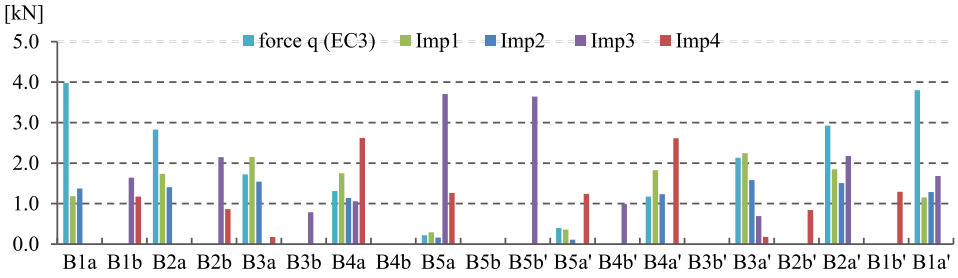

Fig. 11. Axial forces in bar bracing under second order forces – comparison of numerical results for case of bar bracing (BBr_a).

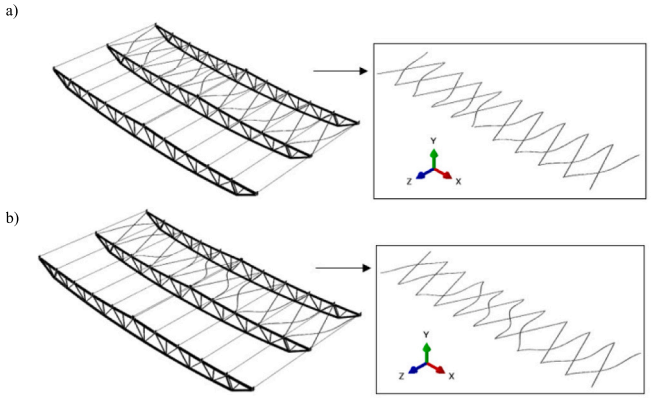

Fig. 12. Deformation of bar bracing (BBr_a case, scale factor = 10): a) Imp1, b) Imp3.

smaller forces in bracing than imperfection with the shape no. 3 and no. 4. This fact suggested that shape no. 1 should not be adopted arbitrary and the analysis of the real shape of the initial imperfections may be required in some cases.

Note, that in all figures in Section 6 only tension forces are demonstrated, because X-shaped bracing considered in the analysis was built from flat bar members (30×4 mm).

Then, in order to compare above values to the exemplary maximum values of the axial forces in the bracing elements, analysis including both second order forces and wind load were performed. Values of axial forces in bar bracing elements obtained in numerical analysis for two cases of the structure and four shapes of the initial imperfections are presented in Fig. 13. The outcomes achieved for the structure subjected to initial imperfection forces and wind loading verified the importance of the previous observations of the axial forces in bar bracing (for the case without wind included). The distribution of the forces with the wind origin dominated the final force distribution in bracing. The least favorable case of the initial imperfection was the case where the extreme axial forces in bar bracing occurred in the same element as the extreme in the case of wind loading (bar bracing element B1a and B1a'). It confirmed previous conclusion that the EC assumptions were safe for the analysed structure. The difference in extreme axial forces in bar bracing between variants of the initial imperfections appeared to oscillate between 4% and 12% for the analysed structure (percentages calculated in reference to the "force q" results). On the other hand, assuming in case BBr number of restrained upper truss chords $m = 4$ (as it could be in real structure in contrast to the analysed part of the roof, where $m = 1$ was assumed), the stabilizing force q increases about 3 times, which gives, according to [1] (see section 3.1), the change of second order forces value from 11% to 36% in comparison to the wind forces. It means that

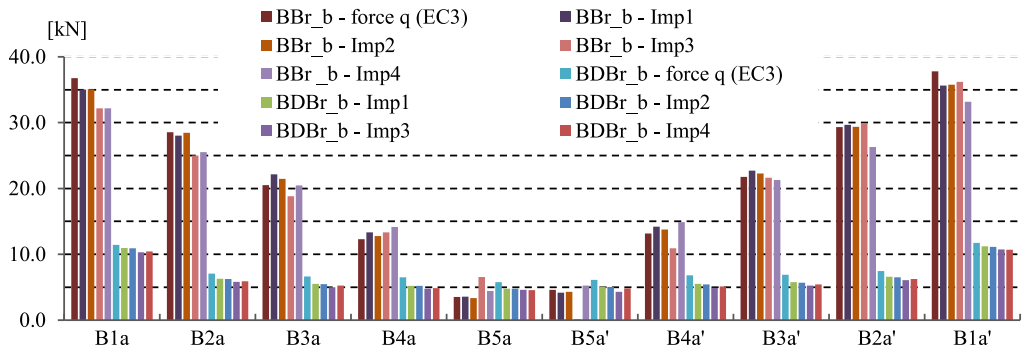

Fig. 13. Axial forces in bar bracing under wind load and imperfections - case of bar bracing (BBr_b) and bar and diaphragm bracing (BDBr_b).

in real structure the imperfections may play more significant role than it occurred in presented analysis of the part of the roof.

In Fig. 14 the comparison between BBr_b case (bar bracing), BDBr_a case (bar and diaphragm bracing, sheeting covers half of the roof) and BDBr_b case (bar and diaphragm bracing, sheeting covers whole roof) is presented. As predicted, sheeting bore significant part of the bracing forces. About 70% decrease of the extremal force in bar bracing in BDBr_b case comparing to BBr_b case was observed, however it should be noticed that the value of the decrease depended strongly on the flexibility of bracings and on the flexibility of the purlin-truss connection, which is the subject of ongoing research.

6.2. Stresses in diaphragm bracing

In the numerical analysis the gravity loads were included as the reactions from purlins to the trusses, which means that the sheeting was not subjected directly to them, only to wind and second order forces. Despite this, stress occurred in the trapezoidal sheeting, which evidenced diaphragm action of cladding. Strength of stressed-skin action depends on, among others, the flexibility of the connections, what is discussed in section 4.2 and 6.3. Here the results of shear stress component (s_{12}) in the sheeting are presented as the most representative stress component for diaphragm action. In Fig. 15, maps of stress in case of wind load and second order forces characterised by initial imperfection no. 1 are given for two cases – diaphragm bracing only (DBr_b) and both diaphragm and bar bracing (BDBr_b). It can be noticed that the area neighbouring to the gable truss (imperfect truss loaded by the wind) was more stressed than the second area, which confirmed that the diaphragm effect impact weakens as the distance from the gable frame increases. The stresses along the path "b" guided along the corrugation in the middle between two trusses (as marked in Fig. 15) were analysed. Taking into account that the connection between sheeting and purlins was built in simplified way (description in section 4.2), the local stress concentration near the sheeting to eave purlins connections was intentionally omitted in the presented results (path "b" was shortened at both ends by 0.16 m). Graph of the shear stress (s_{12}) along the path "b" in case of wind load and second order forces characterised by equivalent stabilizing force q is shown in Fig. 16. It is clearly visible that bar bracing decreased the effort of the cladding (especially in the area close to the eaves). What is more, according to the Eurocode [20], shear stress due to stressed-skin action should not exceed the 25% of the yield strength in order to ensure that bending resistance is crucial before the resistance to stressed skin action is affected. In Fig. 17 the s_{12} stress obtained in path "b" for DBr_b case and structure subjected to wind and second order loads in all imperfection variants (force q, initial imperfections no. 1–4) is presented. Extreme s_{12} stress in the sheeting in case of the analysed structure did not exceed the 25% of the yield strength in any imperfection variant, so the Eurocode condition was fulfilled.

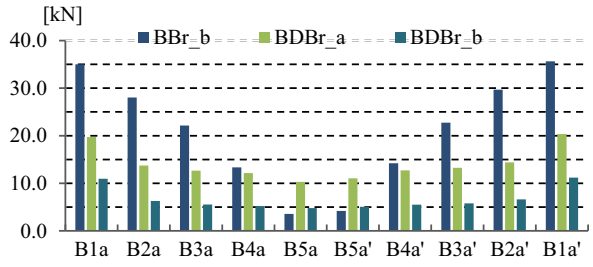

Fig. 14. Axial forces in bar bracing under wind load and imperfection no.1 – three cases of bracing system (BBr_b, BDBr_a and BDBr_b).

6.3. Connections in the bracing system

The stressed-skin effect results in extra forces not only in the sheeting (section 6.2) but also in connections. The capacity of the connections is not within the scope of this paper as the separate subject of ongoing and further studies. However, forces and stresses observed in selected connections in current analysis allow to formulate important conclusions as presented below. Case of diaphragm bracing (DBr_b) and equivalent stabilizing force q was chosen for the discussion, as it was expected to be the case with the biggest diaphragm forces in truss-purlin-sheeting connections.

Screw connections between purlins and sheeting were included numerically using bushing elements. One of the advantage of using bushing element in ABAQUS [25] instead of tie or coupling connection is the possibility to get in relatively simple way the section forces in fasteners. Observed shear forces in purlin-sheeting connections varied with the extreme value equal to 2.6 kN. It means that the screws used to connect purlins and sheeting should be carefully chosen in order to avoid the overloading.

Another connection which need special attention is purlin-truss connection, which in the analysed structure was realised using angle cleat. The L-shaped element geometry was established based on the assortment of the cold-formed element manufacturers, so it was designed to match the "traditional" function (covering function of the sheeting, stressed-skin effect omitted). Whereas in fact purlin-sheeting connection was exposed to extra forces - resulting from diaphragm action of the sheeting, especially high when sheeting is fastened to the main structure only on two sides (only purlin-sheeting connection, without shear connectors between sheeting and trusses). Values of stresses in angle cleats observed in the analysis suggest that standard cleat angles used in traditional approach may not be sufficient in case of stressed-skin design and more stiff one should be used instead. It means that the purlin-truss connection should not be underrated in the design process, which has already been raised in the literature [16].

6.4. Supplement to the discussion of forces in bracing elements

Global deformation in the direction of the wind loads in the midspan

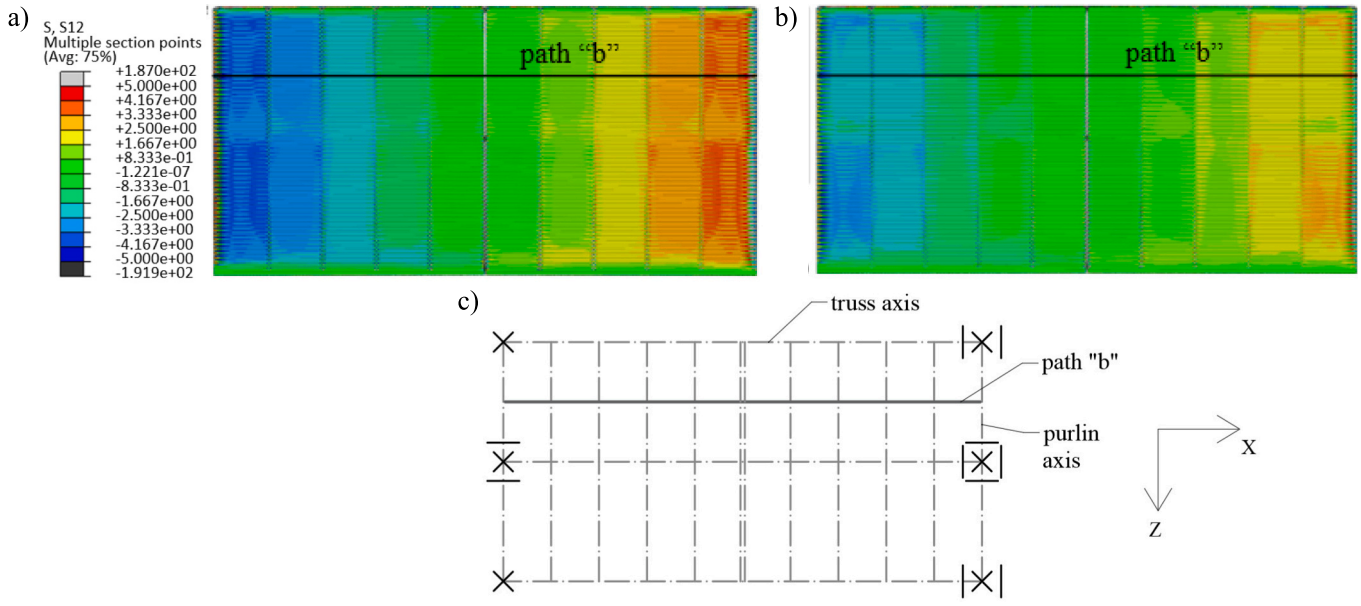

Fig. 15. Stress s_{12} [MPa] – wind load + imperfection no. 1: a) case of diaphragm bracing (DBr_b), b) case of bar and diaphragm bracing (BDBr_b), c) corresponding planar view of the roof.

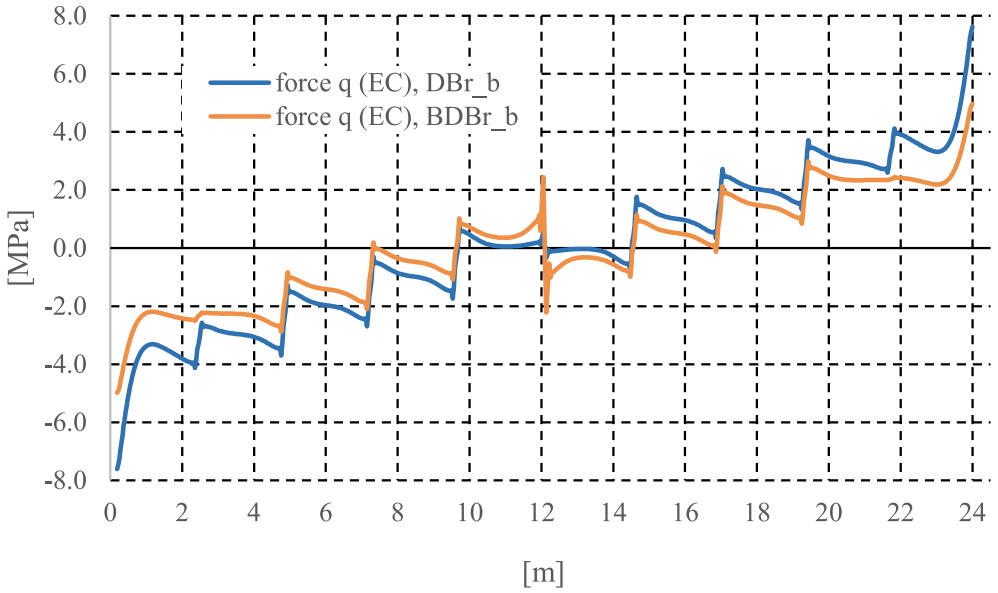

Fig. 16. Stress s_{12} [MPa] along the sheeting, wind load + force q – case of diaphragm bracing (DBr_b) vs. case of bar and diaphragm bracing (BDBr_b).

of the third truss in selected variants of the analysis obtained for beam and shell purlin model were compared. In bar bracing case (BBr) with force *q* applied, the deformation differenced slightly. However in case of diaphragm bracing (DBr), the discrepancies were significant. Difference in global deformation when the sheeting was included suggests the influence on the distribution forces between the structure and the cladding, which is the subject of further research. It means that the analysis concerning forces in bracing in cases with diaphragm taken into account should be treated qualitatively, not quantitatively. However, taken into consideration that the force distribution relies strongly on the stiffness of the bracing (bar/diaphragm/purlin-truss connection), the importance of this issue decreases. On the other hand, it should be treated as a warning in context of the simplified design procedures.

7. Conclusions

Numerical research of three variants of roof bracing including truss imperfection-origin forces were presented. Main conclusions based on the example of the analysed structure are as follows:

- choice of method of taking into account the initial imperfections of the truss girder affected the extreme values and the shape of the stabilizing force in purlins distribution (extreme values according to numerical analysis were about 30% higher than results according to "EC3" procedure, but also significantly smaller than results according to alternative analytical methods).
- "standard" shape of the imperfection (no. 1) should not be assumed arbitrary in the analysis of forces in purlins and the real shape of the initial imperfections should be considered as the biggest force values

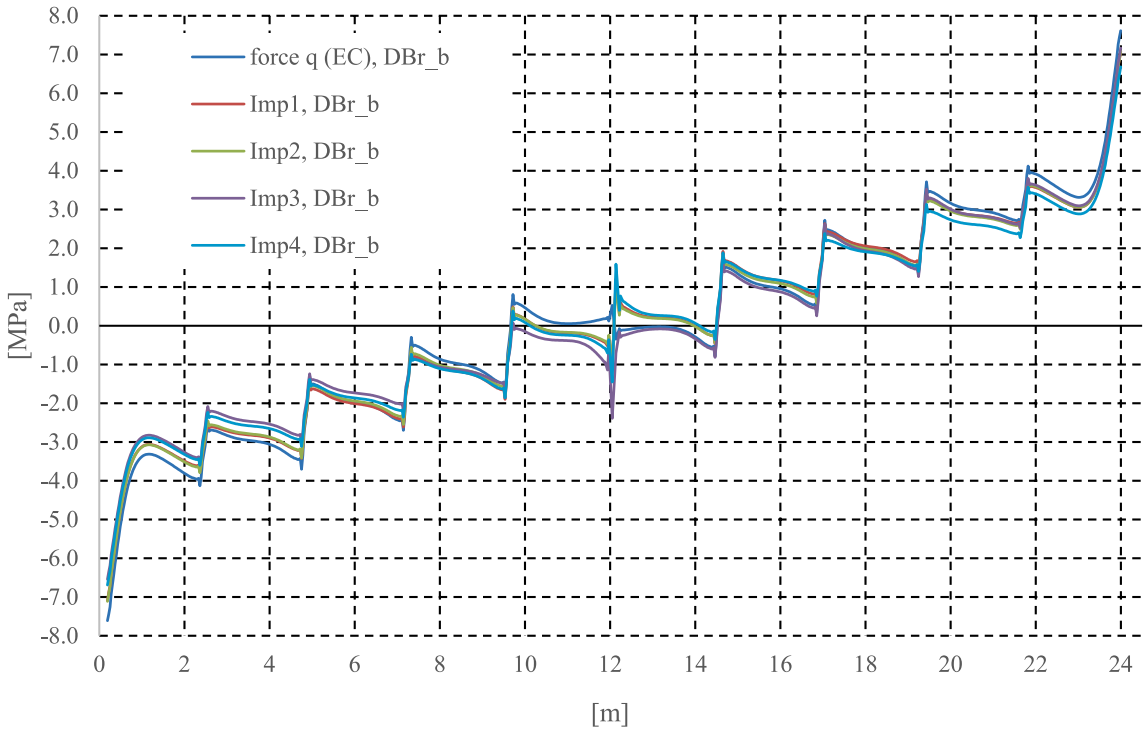

Fig. 17. Stress s_{12} [MPa] along the sheeting, wind load + imperfection – case of diaphragm bracing (DBr_b).

were obtained for the shape no. 3 of the imperfection (more than 2.5 times larger comparing to analytical "EC3" calculations),
- in the calculations of forces in bracings, loading the structure by stabilizing force *q* (calculated according to "EC3") was very conservative approach comparing to implementing "standard" initial imperfection no. 1 directly in the model,
- comparing four shapes of imperfections implemented directly, the biggest forces in bar bracing were obtained for the shape no. 3 of the imperfection, however, when the wind loading was taken into account, the differences in extreme forces did not exceed 12%,
- in bar bracing case (BBr), the ratio between second order forces in bar bracing due to imperfections and forces due to wind loading was equal to 11%; however, in real structure one bracing per a few trusses occurs, hence the significance of the imperfection-induced forces comparing to wind forces increases (a few times), so the initial imperfection may play more significant role than it occurred in presented analysis,
- sheeting may bear significant part of the bracing forces (e.g. about 70% decrease in extreme forces in bar bracing was observed), but the force distribution depends strongly on the flexibility of the bracings and purlin-truss connection,
- when sheeting acts as a diaphragm, extra forces in connections occur, which requires careful design of the connections (and strengthen – if necessary) in order to avoid the overloading.

Nowadays numerical analysis of the entire structure is more and more common in design process. If the 3D numerical model built for the purpose of static calculations exists, it seems reasonable to use it also (after required modifications) for more specific goals as for instance designing bar or diaphragm bracing. In order to recognise the essential components of the numerical analysis (and analytical calculations), intentionally quite sophisticated numerical model of the roof structure was considered. Further research for verification and generalising the results is needed. However, above observations can be treated as a preliminary guidelines for taking into account initial imperfections in numerical analysis of the roof structure with bar and/or diaphragm bracing.

CRediT authorship contribution statement

Natalia Korcz-Konkol: Conceptualization, Data curation, Investigation, Methodology, Software, Visualization, Writing – original draft. **Piotr Iwicki:** Conceptualization, Methodology, Software, Supervision, Writing – review & editing.

Declaration of Competing Interest

The authors declare that they have no known competing financial interests or personal relationships that could have appeared to influence the work reported in this paper.

Data availability

Data will be made available on request.

Acknowledgements

The numerical calculations were performed using the computing resources of CI TASK at Gdańsk University of Technology.

References

[1] EN 1993-1-1: Eurocode 3: Design of steel structures Part 1–1: General rules and rules for buildings.
[2] A. Biegus, D. Czepiżak, Equivalent stabilizing force of the simply supported roof girders including the longitudinal variability of the compression force acting in the restrained chord, Civil Environ. Eng. Rep. 25 (Issue 2) (2017) 43–57, https://doi.org/10.1515/ceer-2017-0019.
[3] A. Biegus, Calculation of lateral bracing for cantilever and multispan girders, Arch. Civil Mech. Eng. 13 (2013) (2013) 99–103.
[4] M. Piątkowski, Experimental research on load of transversal roof bracing due to geometrical imperfections of truss, Eng. Struct. 242 (2021), 112558, https://doi.org/10.1016/j.engstruct.2021.112558.
[5] Iwicki P. (2010) *Stability of roof trusses stiffened by corrugated sheets.* Shell Structures: Theory and Applications, Vol. 2 – Pietraszkiewicz & Kreja (eds), Taylor & Francis Group, London, p. 113-116.
[6] A. Biegus, Trapezoidal sheet as a bracing preventing flat trusses from out-of-plane buckling, Arch. Civil Mech. Eng. 15 (2015) (2015) 735–741.

[7] ECCS - TC7, European Recommendations for the Application of Metal Sheeting Acting as a Diaphragm, Stressed Skin Design, 1995.
[8] A. Lendvai, A.L. Joó, Improvement of stressed skin design procedure based on experimental and numerical simulations, J. Constr. Steel Res. 168 (2020), https://doi.org/10.1016/j.jcsr.2019.105874 (2020), 105874.
[9] M. Gryniewicz, J.K. Szlendak, FEM model of the steel building roof includes stressed skin diaphragm action effects, in: The International Conference on Metal Structures, Zielona Góra, 2016, 2016.
[10] M. Gryniewicz, M. Roberts, J.M. Davies, Testing and analysis of a full-scale steel-framed building including the consideration of structure-cladding interaction, J. Constr. Steel Res. 181 (2021), 106611, https://doi.org/10.1016/j.jcsr.2021.106611.
[11] M. Roberts, J.M. Davies, 3D models of clad steel structures – assumptions and validation, 2022, https://doi.org/10.1201/9781003348443-151.
[12] Nagy Zs, A. Pop, I. Mois, R. Ballok, Stressed skin effect on the elastic buckling of pitched roof portal frames, Structures 2016 (2016), https://doi.org/10.1016/j.istruc.2016.05.001.
[13] Nagy Zs, A. Kelemen, M. Nedelcu, The influence on portal frame buckling of different cladding systems - a comparative numerical study considering stressed skin effect, Thin-Walled Struct. 182 (Part B) (2023), https://doi.org/10.1016/j.tws.2022.110310, 2023, 110310.
[14] N. Korcz, E. Urbańska-Galewska, Influence of fasteners and connections flexibility on deflections of steel building including the stressed skin effect, Techn. Sci. 21 (2) (2018) 131–148, https://doi.org/10.31648/ts.2722.
[15] N. Korcz, E. Urbańska-Galewska, *Influence of sheet/purlin fasteners spacing on shear flexibility of the diaphragm* (2018), MATEC Web of Conferences 219 (2018) 02007.
[16] M. Roberts, J. Davies, Y. Wang, Modern cladding systems for big sheds: the emerging state of the art, Thin-Walled Struct. 175 (2022), 109264, https://doi.org/10.1016/j.tws.2022.109264.
[17] M. Roberts, J.M. Davies, Y. Wang, Numerical analysis of a clad portal frame structure tested to destruction, Structures 33 (2021) 3779–3797, https://doi.org/10.1016/j.istruc.2021.06.098.
[18] J. Davies, M. Roberts, Y. Wang, Stressed skin theory and structure cladding interaction: safety concerns with big sheds, Thin-Walled Struct. 169 (2021), 108415, https://doi.org/10.1016/j.tws.2021.108415.
[19] N. Korcz-Konkol, P. Iwicki, Corrugated sheeting as a member of a shear panel under repeated load—experimental test, Materials 13 (18) (2020) 4032, https://doi.org/10.3390/ma13184032.
[20] K. Rzeszut, A. Gastecki, A. Czajkowski, Parameter identification in FEM models of thin-walled purlins restrained by sheeting, in: Recent advances in computational mechanics: Proceedings of the 20th International Conference on Computer Methods in Mechanics (CMM 2013), Poznań, Poland, 2014.
[21] T. Höglund, Stabilization by Stressed Skin Diaphragm Action, 2002. SBI.
[22] EN 1993-1-3: Eurocode 3: Design of steel structures Part 1–3: General rules - Supplementary rules for cold-formed members and sheeting.
[23] N. Korcz-Konkol, P. Iwicki, Stabilizing forces in trapezoidal sheeting used as a part of the bracing system, ce/papers 4 (2021) 2242–2248, https://doi.org/10.1002/cepa.1545.
[24] P. Iwicki, Selected Problems of Stability of Steel Structures, Wydawnictwo Politechniki Gdańskiej, Gdańsk, 2010.
[25] ABAQUS, Theory Manual, Version 6.8, Hibbit, Karlsson & Sorenses Inc, 2008.
[26] S. Shayan, K.J.R. Rasmussen, H. Zhang, On the modelling of initial geometric imperfection of steel frames in advanced analysis, J. Constr. Steel Res. 98 (2014) (2014) 167–177, https://doi.org/10.1016/j.jcsr.2014.02.016.
[27] N. Korcz-Konkol, P. Iwicki, Stability of roof trusses stiffened by trapezoidal sheeting and purlins, MATEC Web Conf. 219 (2018).